Table S1, related to Figure 1.

Case #	WHO grade[a]	Age[b]	Gender[c]	Tumor location[d]	KPS[e]	GBM subtype
74	IV	74	M	L frontal, parietal	40%	classic
194	IV	71	M	L parietal, temporal	80%	classic
216	IV	67	F	L parietal, occipital	40%	not determined
269	IV	65	F	R frontal	ND	classic
317	IV	71	F	R temporal	50%	not determined
356	IV	74	M	R frontal, temporal, insula	70%	classic
384	IV	45	M	R parietal, temporal, midbrain	50%	not determined
391	IV	54	F	R parietal, temporal	50%	mesenchymal
397	IV	58	F	L parietal, frontal	90%	R132H - proneural
435	IV	34	M	L parietal, frontal	50%	not determined
442	IV	68	M	R frontal, temporal, parietal	50%	not determined
485	IV	67	M	R parietal, temporal	60%	classic
496	IV	57	F	R parietal, temporal	70%	classic
498	IV	17	F	R frontal, parietal, temporal	30%	classic
510	IV	56	M	R parietal	50%	not determined
522	IV	48	M	L temporal	100%	R132H - proneural
592	IV	45	M	L parietal, frontal	80%	proneural
1103	IV	54	M		ND	mesenchymal
1124	IV	63	M	R parietal, temporal, insula	50%	Classic

[a], non-neoplastic; II, low-grade astrocytoma; III, anaplastic astrocytoma; IV, glioblastoma (GBM).

[b], Age at diagnosis was calculated from date of birth to date of surgery.

[c], M, Male; F, Female.

[d], L, Left; R, Right.

[e], Karnowsky Performance Status. Patients are classified according to their functional impairment level, where 100% as normal and 0% as dead.

Table S2, related to Figure 1

Name	PTEN Expr	FGFR1 Expr	FGFR2 Expr	FGFR3 Expr	PTEN Mutation	PTEN protein	Radiation Response
GSC295	6.9	15.3	15.3	15.3			Sensitive
GSC2	6.3	8.9	8.9	8.9			Resistant
GS10-6	6.2	10.9	10.9	10.9			Resistant
GSC296	5.8	14.1	14.1	14.1			Resistant
GS5-22	5.7	11.5	11.5	11.5			Sensitive
GSC112	4.7	6.9	6.9	6.9			Sensitive
GS4-16	4.7	11.0	11.0	11.0			Resistant
GS3-25	4.6	7.8	7.8	7.8			intermediate
GSC304	4.5	12.4	12.4	12.4			Resistant
GSC300	4.0	10.6	10.6	10.6			Resistant
GS7-2	3.7	15.8	15.8	15.8			Resistant
GSC264	3.6	17.7	17.7	17.7			intermediate
GS7-11	3.4	4.2	4.2	4.2	Missense	I33F	Sensitive
GSC107	3.4	5.9	5.9	5.9			Resistant
GS7-10	3.2	6.4	6.4	6.4	Missense	Y68H	intermediate
GSC289	3.1	17.8	17.8	17.8			intermediate
GSC293	3.0	6.1	6.1	6.1			Sensitive
GSC280	2.9	6.9	6.9	6.9	Splice Site		intermediate
GSC34	2.8	11.2	11.2	11.2			Resistant
GSC16	2.6	5.5	5.5	5.5			intermediate
GSC275	2.4	8.4	8.4	8.4	Missense	D22G	intermediate
GSC17	2.4	0.1	0.1	0.1	In Frame del	del198M	Resistant
GSC240	2.4	6.0	6.0	6.0			intermediate
GSC248	2.3	10.5	10.5	10.5			intermediate
GS4-23	2.3	13.4	13.4	13.4	Missense	M134I	Sensitive
GSC272	2.2	5.7	5.7	5.7			Sensitive
GS8-18	2.1	10.4	10.4	10.4			Sensitive
GSC268	2.0	6.8	6.8	6.8			Resistant
GSC28	1.9	8.4	8.4	8.4			Sensitive
GS8-11	1.8	2.2	2.2	2.2			Sensitive
GS7-15	1.7	6.9	6.9	6.9			Resistant
GS2-14	1.7	4.9	4.9	4.9			Sensitive
GSC20	1.2	7.2	7.2	7.2			Sensitive
GSC231	1.2	9.5	9.5	9.5			Sensitive
GSC262	1.1	10.1	10.1	10.1			Sensitive
GSC23	0.6	16.4	16.4	16.4			Resistant
GS3-28	0.4	6.6	6.6	6.6			Resistant
GSC11	0.2	16.7	16.7	16.7			Resistant
GSC285	0.0	9.8	9.8	9.8			intermediate
GS6-27	0.0	8.4	8.4	8.4			Resistant
GSC282	0.0	7.5	7.5	7.5			Sensitive
GSC236	0.0	10.7	10.7	10.7			Sensitive
GSC267	0.0	14.3	14.3	14.3			Sensitive
GSC274	0.0	3.8	3.8	3.8			Sensitive

Bold line indicated the median expression value of PTEN (2.5) for all cell lines in this RNAseq experiment based on RPKM values from normalized transcriptome sequencing.

Table S3, related to all Figures with cell data.

Cells	FGFR2	PTEN wild-type	PTEN Y240F	Heter_expr
U87	Not detectable	-	-	FGFR2, WT-or YF-PTEN
HK281	+	-	-	WT-or YF-PTEN
				Endogenous
TS528	+	+	-	FGFR2, WT-PTEN
GBM patient-derived cells	+	+	-	FGFR2, WT-PTEN
Mouse WT primary spheres	+	+	-	FGFR2, WT-PTEN
Mouse YF primary spheres	+	-	+	FGFR2, YF-PTEN

YF: Y240F mutant PTEN; Heter_expr: Heterologous expression

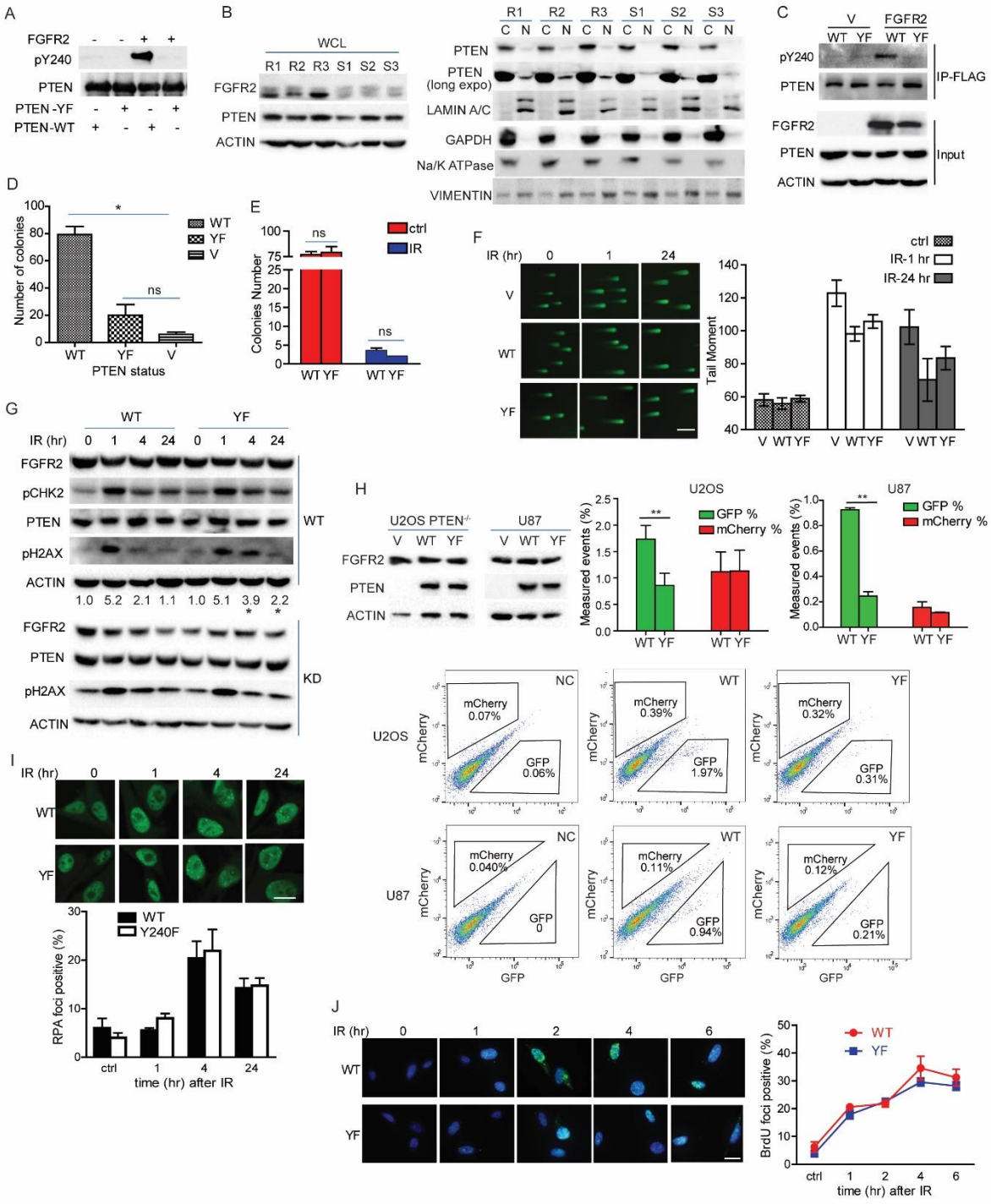
A
FGFR2
pY240
PTEN
PTEN -YF
PTEN-WT
B
WCL
R1 R2 R3 S1 S2 S3
FGFR2
PTEN
ACTIN
R1 R2 R3 S1 S2 S3
C N
PTEN
PTEN (long expo)
LAMIN A/C
GAPDH
Na/K ATPase
VIMENTIN
C
V FGFR2
WT YF WT YF
pY240
PTEN
IP-FLAG
FGFR2
PTEN
ACTIN
Input
D
Number of colonies
WT
YF
V
PTEN status
E
Colonies Number
ctrl
IR
WT YF WT YF
F
IR (hr) 0 1 24
V
WT
YF
Tail Moment
ctrl
IR-1 hr
IR-24 hr
V WT YF V WT YF V WT YF
G
WT YF
IR (hr) 0 1 4 24 0 1 4 24
FGFR2
pCHK2
PTEN
pH2AX
ACTIN
1.0 5.2 2.1 1.1 1.0 5.1 3.9 2.2
KD
H
U2OS PTEN-/-
U87
V WT YF V WT YF
Measured events (%)
GFP %
mCherry %
U2OS
U87
WT YF WT YF
NC
WT
YF
mCherry 0.07%
GFP 0.06%
mCherry 0.39%
GFP 1.97%
mCherry 0.32%
GFP 0.31%
mCherry 0.040%
GFP 0
mCherry 0.11%
GFP 0.94%
mCherry 0.12%
GFP 0.21%
I
IR (hr) 0 1 4 24
WT
YF
RPA foci positive (%)
WT
Y240F
ctrl 1 4 24
time (hr) after IR
J
IR (hr) 0 1 2 4 6
WT
YF
BrdU foci positive (%)
WT
YF
ctrl 1 2 4 6
time (hr) after IR

Figure S1, related to Figure 1

(A) In vitro kinase assay was performed by incubating recombinant FGFR2 with recombinant purified GST-PTEN (WT and Y240F (YF)), followed by probing with anti-pY240-PTEN antibody and PTEN antibody. **(B)** Three representative cells from radiation sensitive or resistant group (Figure 1D) were analyzed for PTEN expression and localization. Left panel represents PTEN expression level in whole cell lysates; right panel indicates equal cell equivalents of nuclear (N) and cytoplasm (C) fractions from these cells immunoblotted for PTEN and FGFR2. R1-3, 3 radiation resistant cells; S1-3, 3 radiation sensitive cells. **(C)** U87 cells transfected with FGFR2 or empty vector (V) along with WT-or YF-PTEN were blotted for the presence of pY240-PTEN. **(D)** Colony numbers from WT-, YF-PTEN cells and vector control (V) cells after treatment with 10 Gy irradiation. **(E)** Bar graph shows colony numbers of different treatment groups in the absence of FGFR2. **(F)** Images show comet assay for U87 cells reconstituted with empty vector (V), WT- or YF-PTEN in the absence of FGFR2. Bar graph at right shows quantification of tail moment. Scale bar, 500 µm. **(G)** Wild type (WT) or kinase dead (KD) FGFR2 was overexpressed in U87 cells reconstituted with WT-or YF-PTEN. Cells were treated with 10 Gy IR and pH2AX was examined at indicated times. Numbers at the bottom indicate ratio of pH2AX levels relative to time 0 after normalization to actin, calculated as mean ± SD from three independent experiments, *$p<0.05$ was generated by comparing WT- and YF-PTEN samples at the same time point. **(H)** U2OS cells CRISPR/Cas9 edited for PTEN or U87 cells were reconstituted with empty vector (V), WT- or YF-PTEN along with FGFR2 (left top). DNA repair efficiency using traffic light assay was determined by flow cytometry, with percentage of GFP-positive cells indicating HR efficiency and mCherry-positive cells indicating NHEJ efficiency. Representative flow plots are shown (bottom) and bar graph indicating quantification of flow cytometry data (right top). NC, negative control, where no DNA damage was induced by I-SceI. **(I)** WT- or YF-PTEN U87 cells were treated with 10 Gy IR and RPA32 foci were detected at indicated times by immunostaining. Representative images and quantification of foci positive cells are shown. Scale bar, 25 µm. **(J)** Cells treated and analyzed the same as (**I**) for BrdU foci. Scale bar, 25 µm. Error bars in this figure represent SD from three independent experiments. ns, not significant, *$p < 0.05$, **$p < 0.01$.

Table S4, related to Figure 2.

Name	Source	Cell type	In vitro growth	In vivo growth	FGFR2	PTEN
GBM 39	David James UCSF	Neurosphere (GBM xenograft)	moderate	moderate	-	+
GBM 6	David James UCSF	Neurosphere (GBM xenograft)		slow	-	+
GBM 1600	Dr. Mischel UCLA		fast		-	+
HK 281	Dr. Kornblum UCLA	Human neurosphere	fast	fast	+	-
GSC 11	Fred Lang, MD Anderson	Glioma stem cell	fast		-	-
GSC 23	Fred Lang, MD Anderson		fast		+	-
TS528	Dr. Brennan MSKCC	Glioma stem cell	fast		+	+
TS543	Dr. Brennan MSKCC	Glioma stem cell	fast	fast	-	+
TS576	Dr. Brennan MSKCC	Glioma stem cell	fast	fast	-	+
TS600	Dr. Brennan MSKCC	Glioma stem cell	fast	moderate	-	-
GSC2	Erik Sulman MD Anderson	Glioma stem cell	moderate	moderate	+	+
GS10-6	Erik Sulman MD Anderson	Glioma stem cell	slow		+	+

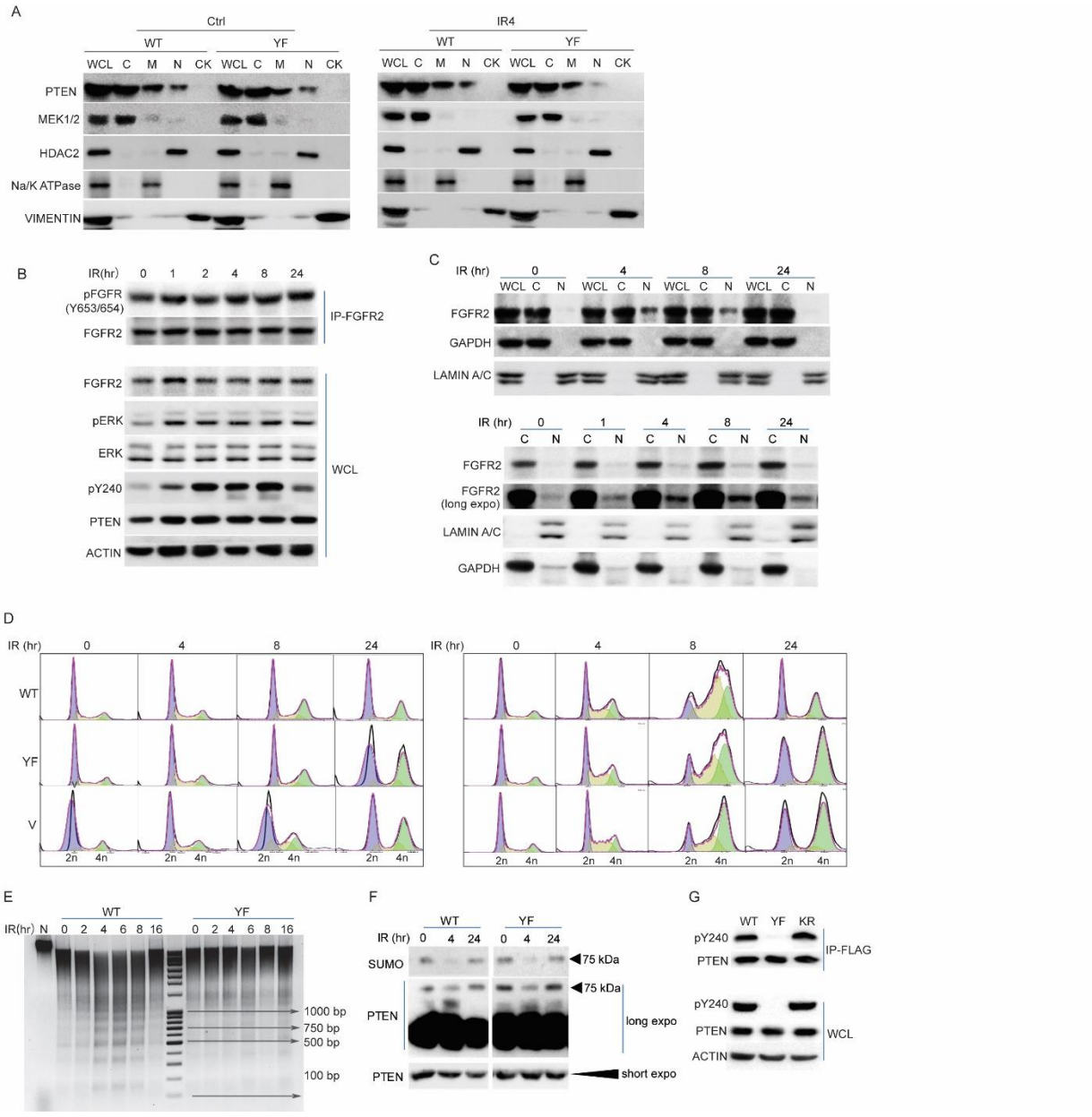
A
Ctrl
IR4
WT
YF
WCL C M N CK WCL C M N CK
PTEN
MEK1/2
HDAC2
Na/K ATPase
VIMENTIN
B
IR(hr) 0 1 2 4 8 24
pFGFR (Y653/654)
FGFR2
IP-FGFR2
FGFR2
pERK
ERK
pY240
PTEN
ACTIN
WCL
C
IR (hr) 0 4 8 24
WCL C N
FGFR2
GAPDH
LAMIN A/C
IR (hr) 0 1 4 8 24
C N
FGFR2
FGFR2 (long expo)
LAMIN A/C
GAPDH
D
IR (hr) 0 4 8 24
WT
YF
V
2n 4n
E
WT
YF
IR(hr) N 0 2 4 6 8 16 0 2 4 6 8 16
1000 bp
750 bp
500 bp
100 bp
F
WT
YF
IR (hr) 0 4 24 0 4 24
SUMO
75 kDa
PTEN
75 kDa
long expo
PTEN
short expo
G
WT YF KR
pY240
PTEN
IP-FLAG
pY240
PTEN
ACTIN
WCL

Figure S2, related to Figure 3

(A) U87 cells reconstituted with WT-PTEN along with FGFR2 were treated with IR (10 Gy) and then examined for PTEN subcellular localization by western blot. WCL, whole cell lysates, C, cytoplasm, N, nuclear, M, membrane, CK, cytoskeleton. **(B)** Cells lysates from **(A)** were prepared followed by immunoprecipitation with anti-FGFR2 antibody and western blot examination of phosphorylation of FGFR2 (Tyr653/654) in IP products and phosphor-ERK in whole cell lysates. **(C)** cytoplasm (C) and nuclear fractions (N) were prepared and were examined for FGFR2. Long expo, longer exposure time. **(D)** Cell cycle profiles were examined from U87 cells (left) or HK281 cells (right) reconstituted with V or WT- or YF-PTEN along with FGFR2 after IR treatment at the indicated times. **(E)** Micrococcal nuclease assay was performed using U87cells reconstituted with WT- or YF-PTEN along with FGFR2 after IR treatment at the indicated times. N, non-IR control. **(F)** Cells were treated with or without IR at 10 Gy, cell lysates were prepared followed by immunoprecipitation with anti-PTEN antibody. SUMOylation was evaluated by anti-SUMO 2/3 antibody and PTEN-HRP antibody. Long expo, longer exposure time; short expo, shorter exposure time. **(G)** 293T cells transfected with Flag-tagged WT- or YF- or K254R (KR)-PTEN along with FGFR2 were examined for phosphorylation of Y240 PTEN by western blot.

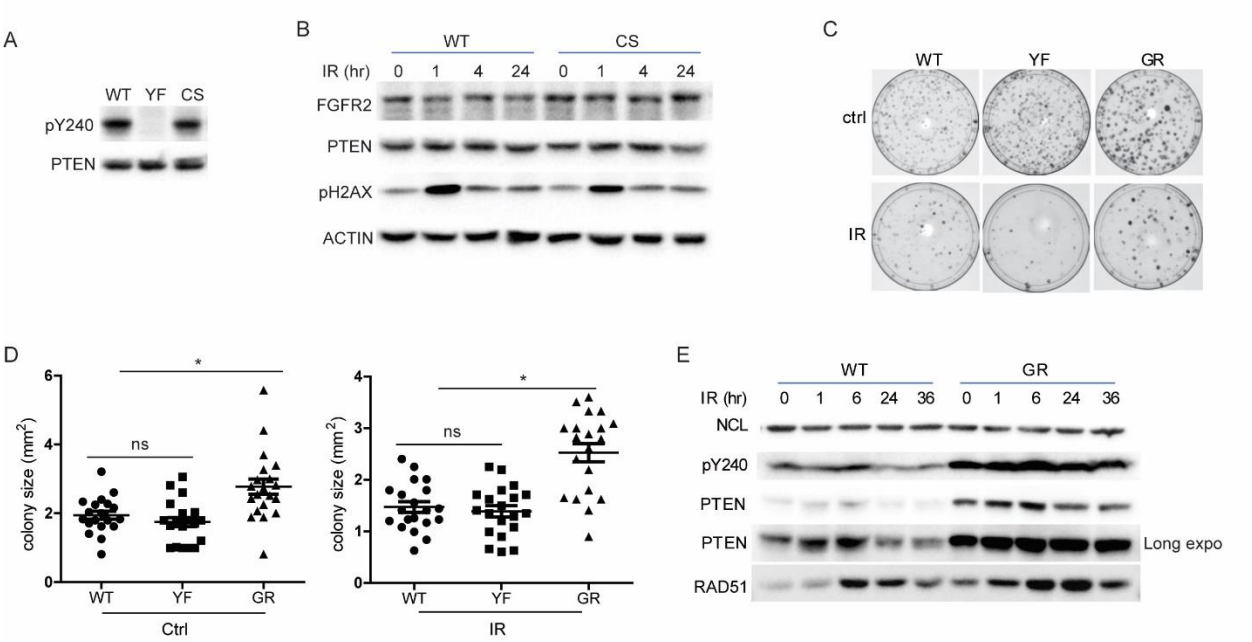

Figure S3, related to Figure 4

(A) U87 cells reconstituted with WT-, YF- or C124S (CS)-PTEN were examined for phosphorylation of Y240 PTEN by western blot. **(B)** Cells from (A) were treated with 10 Gy IR and analyzed for pH2AX at indicated times. **(C)** U87 cells reconstituted with WT-, YF- or GR-PTEN were treated with 10 Gy IR and were analyzed for colony formation, and representative images are shown. **(D)** Colony size was determined by Keyence software and graphed as shown. ns, not significant; Data represent mean ± SD from three independent experiments. *$p < 0.05$. **(E)** U87 cells reconstituted with WT-, GR-PTEN along with FGFR2 were treated with 10 Gy IR and chromatin-bound protein isolated at indicated times post IR was immunoblotted for pY240 PTEN and RAD51.

A

Method	Structure Overlap (%)	RMSD	Fragment Score[1]	Topology Score[2]	Match Size	TM-score	Z-Score
CLICK	60.40	2.01	0.94	0.24	32	-	5.3
mTM-align	-	2.11	-	-	29	0.34	-
RaptorX	-	2.41	-	-	22	0.30	-
SPalign	60.38	1.96	-	-		0.40	

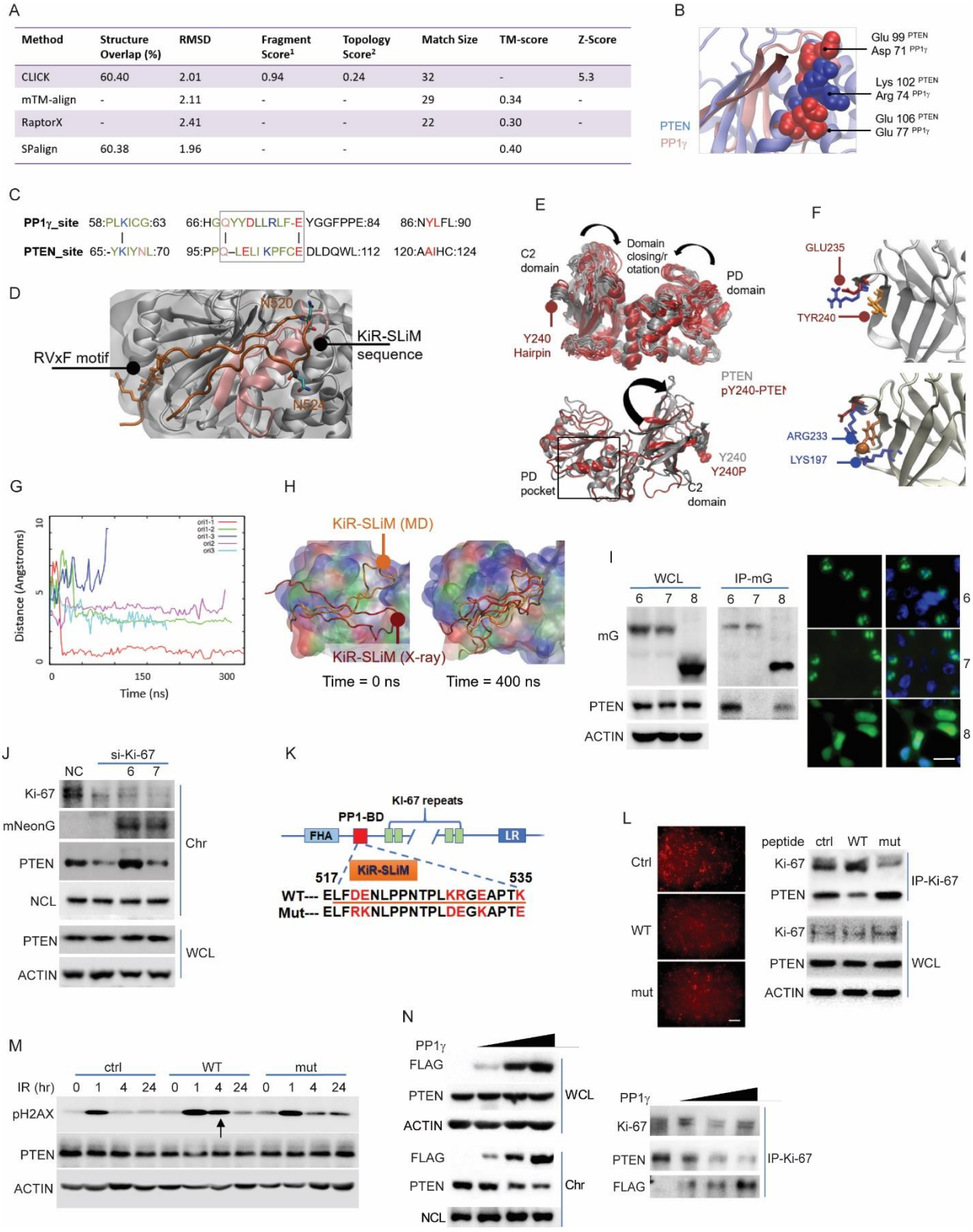

Figure S4, related to Figure 5

(A) The binding pocket for the KiR-SLiM of PP1γ and PTEN showed high 3D structure similarity (<2.5Å) according to different structural alignment methods (CLICK, SPalign, RaptorX, mTM-align) according to different structural alignment methods (CLICK, SPalign, RaptorX, mTM-align) (Brown et al., 2016; Dong et al., 2018; Nguyen et al., 2011; Wang et al., 2013). All methods identified a helix motif **(B)** with a 11-mer sequence of chemically-conserved positions highlighted with a box **(C),** along with two neighboring beta-sheets, which together form the binding site for Ki-67. Note the identically charged residues in **(B)**. **(D)** Pose illustrating close-up view of the PP1γ (PDB entry: 5J28) -Ki-67 interaction. Compared with the interaction of pY240-PTEN (Figure 5I), the KiR-SLiM sequence is flipped but retains key asparagines and other polar/charged residues in similar positions within the binding cleft. **(E)** Comparison of simulations of native (grey) and pY240-PTEN (red) show that phosphorylation favors the closure of the isoprenoid binding cleft (above) and increases the accessibility of the PD binding pocket (below). **(F)** Close-up view of the TYR240 phosphorylation site. While TYR240 forms stable H-bonds with GLU235 and ARG233 in native PTEN, upon phosphorylation these contacts are broken and substituted by interactions between the negatively charged pTYR240 with LYS197 and ARG233 (right). **(G)** Multiple short unbiased trajectories in which the Ki-67 fragment was randomly placed around pY240-PTEN were run and then Ki-67 was directly docked in a similar pose as that observed for its interaction with PP1γ. To prepare the pY240-PTEN structure, short MD runs were performed using the unphosphorylated protein as control. Average distance between Ki-67 and the PD binding pockets seen in different replica trajectories for blind docking; The trajectory in red corresponds to the spontaneous binding event of Ki-67 to conserved phosphatase domain pocket shown in Figure 5H, 5I. **(H)** Comparison of the X-ray guided Ki-67 docking pose (red) with the spontaneous MD complex (orange) at 0 and 400 ns time; note how the KiR-SLiM sequence docked as in the crystal tends to reorient acquiring a similar arrangement as in the simulation complex. **(I)** Ki-67 truncations 6, 7 and 8 (Figure 5G) was co-transfected with PTEN in 293T cells followed by IP with mNeonGreen nAb and western blotted with mNeonGreen (mG) and PTEN antibody (left panel). Representative images showing the localization of truncations 6, 7 and 8 (right panel). Scale bar, 50 μm. **(J)** Rescue experiment was performed by expressing Ki-67 truncation 6 and 7 (Figure 5G) in U87-GR-PTEN cells knocked down for Ki-67 (siRNA-2) expression. PTEN chromatin loading was detected by western blot. NC, si-scramble, non-specific control. **(K)** WT and mutant Ki-67 peptides containing the KiR-SLiM motif were synthesized. **(L)** GR-PTEN U87 cells transfected with control peptide (R-phycoerythrin, with red fluorescence) alone, or together with Ki-67 peptides (WT or mutant) at 1:5 ratio. Representative pictures indicate the transfection efficiency (left panel). Cell lysates were collected 6 hr after transfection and co-immunoprecipitation was performed using Ki-67 antibody. Western blot (right panel) showed WT peptide transfection decreased PTEN and Ki-67 interaction. wt, wild type Ki-67 peptide; mut, mutant Ki-67 peptide. Scale bar, 500 μm **(M)** U87 cells reconstituted with WT-PTEN along with FGFR2 were transfected with control, WT or mutant Ki-67 peptides followed by IR (10Gy) treatment. pH2AX was examined at indicated times after IR. **(N)** U87-GR-PTEN cells were transfected with increasing amount of PP1γ and cell lysates were used to perform co-immunoprecipitation using Ki-67 antibody (right). Chromatin binding of PTEN and PP1γ and interaction between Ki-67 and PTEN or PP1γ were evaluated by western blot (left).

Table S5, related to Figure 5

Simulations	Starting conformation	Time (ns)	Observed events
PTEN phosphorylation	Native PTEN	250	Hinge-bending motions of the PD and C2 domains
	pY240-PTEN	950	Increased motions with closure of the PD / C2 catalytic cleft
PTEN-KI-67 interaction (Blind docking)	Orientation 1 (3X)	325	Tumbling and docking to PD pockets
		275	Weak lateral interactions
		75	Increasing separation
	Orientation 2	250	Weak lateral interactions
	Orientation 3	175	Weak lateral interactions
PTEN-KI-67 complex	MD spontaneous complex (2X)	1075	Stable binding through KiR-SLiM
		925	Stable binding through KiR-SLiM
	X-ray guided complex (2X)	400	Reorientation to blind-docking pose
		425	
Total simulation time (μs)		5.1	

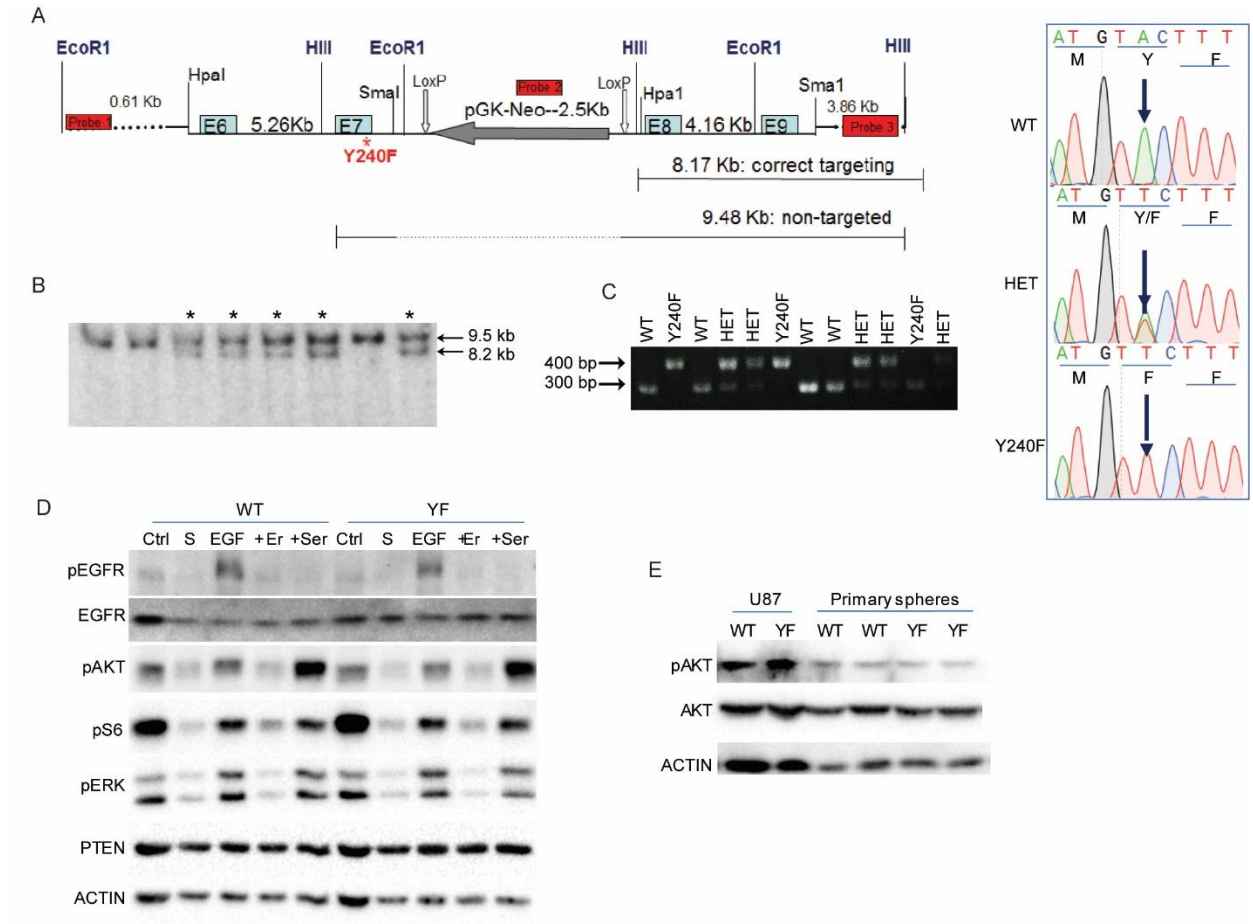

Figure S5, related to Figure 6.

(A) Schematic representation of *Cdkn2a* null; Y240F *Pten* knock-in strategy. Box E6, E7, E8, E9 represent *Pten* exons. pGK-Neo-2.5K denotes neomycin resistance selection cassette. Y240F point mutation and Hind III restriction site adjacent to E7 were introduced by PCR in the targeting vector. **(B)** Southern analysis of ES cell clones. Hind III-digested genomic DNA was hybridized with probe 3. *Indicates correctly targeted clones, which show the presence of an 8.2 Kb fragment, while 9.5 Kb indicates non-targeted events. **(C)** Genotyping PCR reactions were performed using tail DNA followed by RsaI digestion. WT mice showed a single band of 300 bp, while mice with the Y240F knock-in allele displayed a 400 bp product (loss of RsaI restriction site present in WT allele). Genotyping results were ultimately confirmed by sequencing (right). **(D)** Mouse embryo fibroblasts (MEFs) were prepared from E12.5 WT and Y240F embryos as described (Durkin et al., 2013). Cells were serum starved for 16 hours followed by treatment with EGF, EGF+ 5 μM Erlotinib (EGFR inhibitor) or 10% FBS stimulation. Cell lysates were collected 30 min after stimulation and AKT and EGFR-MAPK/ERK pathways activation were examined. S, serum starvation; EGF, 10 ng/mL; +Er, EGF plus 5 μM Erlotinib; +ser, stimulated with 10%FBS. **(E)** Primary neurospheres were prepared as described and PTEN lipid phosphatase activity was compared between WT and Y240F by assessing AKT activation.

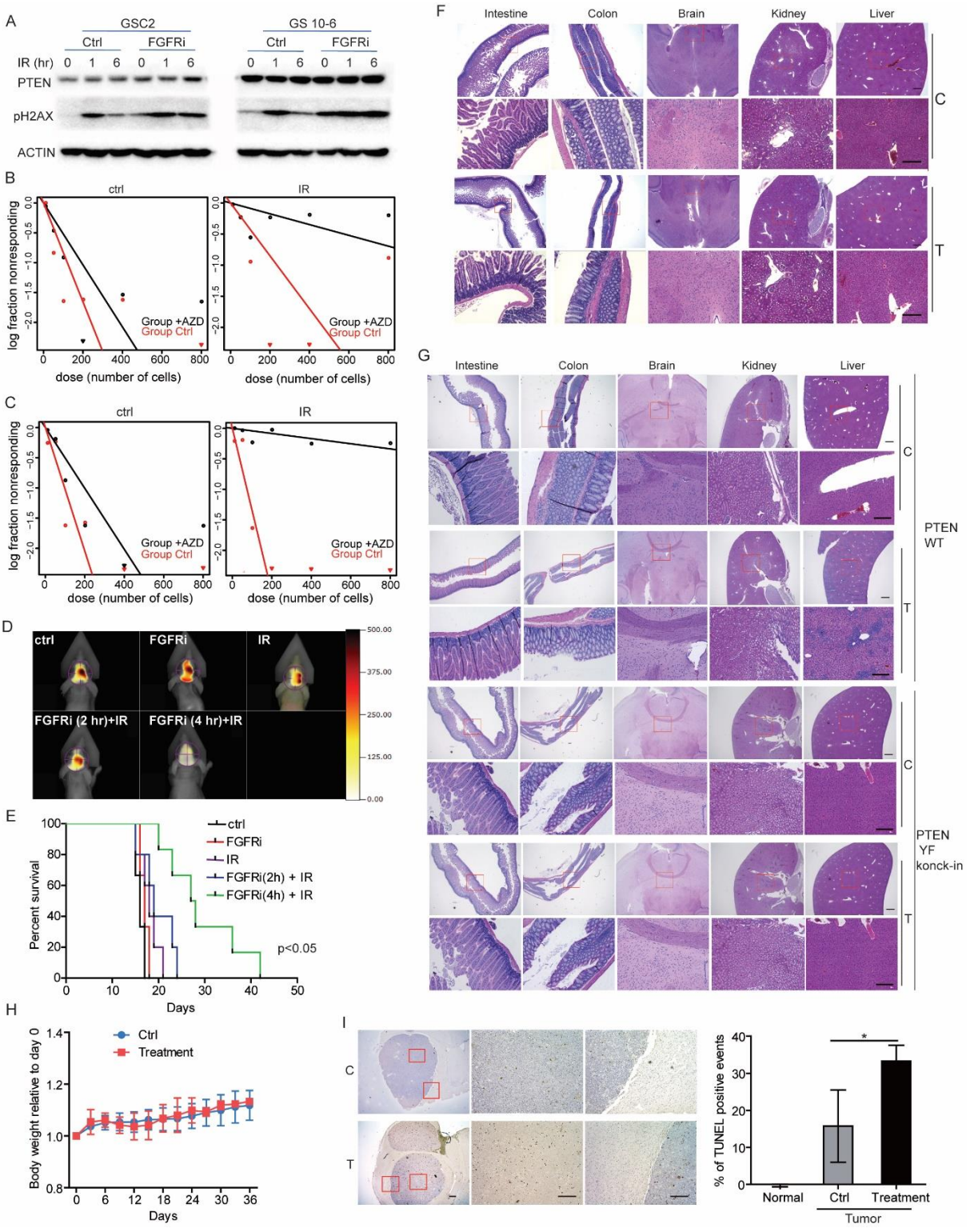
A
GSC2
GS 10-6
Ctrl
FGFRi
IR (hr) 0 1 6 0 1 6
PTEN
pH2AX
ACTIN
B
ctrl
IR
log fraction nonresponding
Group +AZD
Group Ctrl
dose (number of cells)
C
D
ctrl
FGFRi
IR
FGFRi (2 hr)+IR
FGFRi (4 hr)+IR
E
Percent survival
Days
ctrl
FGFRi
IR
FGFRi(2h) + IR
FGFRi(4h) + IR
p<0.05
F
Intestine
Colon
Brain
Kidney
Liver
C
T
G
PTEN WT
PTEN YF konck-in
H
Body weight relative to day 0
Ctrl
Treatment
Days
I
% of TUNEL positive events
Normal
Ctrl
Treatment
Tumor

Figure S6, related to Figure 7.

(A) GSC2 and GS 10-6 cells were treated with or without FGFR inhibitor, AZD4547 (1 μM), for 16 hr and then irradiated at 5 Gy. Cell lysates were prepared for detection of pH2AX by western blot. **(B)** GS 10-6 cells, pre-treated with or without AZD4547, were irradiated at 5 Gy and were analyzed for survival by limiting dilution assay. **(C)** GSC2 cells were treated and analyzed as (**B**). **(D)** GSC2 cells ($0.5x10^6$) were intracranially injected into immunodeficient mice and after tumor establishment mice were administrated AZD4547 by gavage combined with IR for three cycles starting from day 14 after post engraftment (see Figure 7B). Representative images taken at day 18 are shown. **(E)** Kaplan-Meier analysis of mice survival are shown. Ctrl, treated with vehicle; FGFRi, treated with 50 mg/Kg AZD4547; IR, treated with 2.5 Gy IR; FGFRi (2 hr)-IR, treated with 2.5 Gy IR after 2 hr of AZD treatment; FGFRi (4 hr)-IR, treated with 2.5 Gy IR after 4 hr of AZD treatment. **(F)** As in Figure 7B-F, immunodeficient mice (nu/nu), from the same vendor as Figure 7, were subjected to IR treatment four hours after AZD4547 administration for 3 consecutive days. Representative images show H&E staining of sections from major organs 24 hr after last treatment, including intestine, colon, brain, kidney and liver. C, non-treated; T, treated. Scale bar, 200 μm. **(G)** WT- and YF- *Pten* knock-in mice (C57BL/6J) were treated with IR 4 hr after AZD4547 administration for 3 consecutive days. Representative images show H&E staining of sections from major organs 24 hr after treatment, including intestine, colon, brain, kidney and liver. Scale bar, 200 μm. **(H)** Body weight change of mice from **(F)** was monitored after treatment over time up to 36 days. **(I)** Immunodeficient mice were orthotopically injected with HK281-WT-PTEN cells ($2.0x10^5$ cells per mouse). Tumor formed two weeks after injection as monitored by FMT signal. Mice with tumors were treated with IR four hours after AZD4547 administration for 3 consecutive days. Brains were collected 24 hr after treatment followed by TUNEL staining. Bar graph indicates quantification of TUNEL positive cells in tumor area and surrounding normal brain. Scale bar, 100 μm. Error bars represent SD from three independent evaluations, $*p < 0.05$.

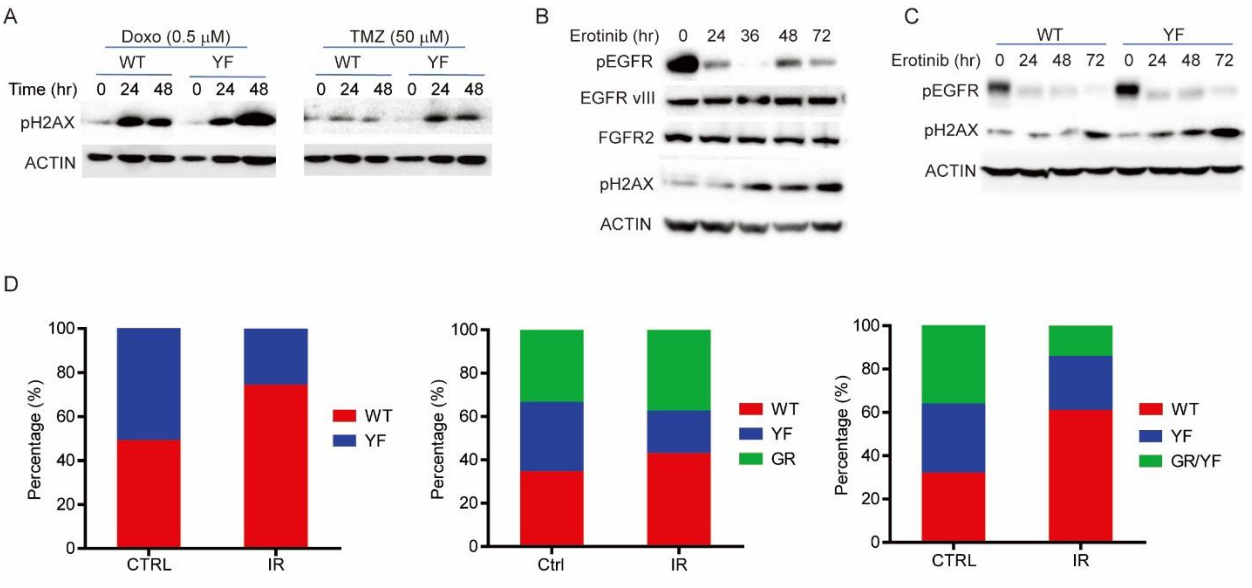

Figure S7, related to Figure 7.

(A) U87 cells reconstituted with WT or Y240F PTEN along with FGFR2 were treated with 0.5 μM doxorubicin (Dox) or 50 μM temozolomide (TMZ) for the indicated time. pH2AX was detected by western blot analysis. **(B)** GBM39, a patient-derived EGFRvIII-expressing xenograft model, was treated with 5 μM EGFR inhibitor, Erlotinib, for the indicated times. **(C)** U87 cells reconstituted with WT- or YF-PTEN along with EGFRvIII were treated with 5 μM Erlotinib for the indicated time. pH2AX was detected by immunoblot analysis. **(D)** HK281 cells reconstituted with WT-, YF-, GR-, or Y240F/G129R (GR/YF)-PTEN were stably labeled with RFP, BFP, GFP and GFP, respectively, and were mixed in equal ratios as shown. Mixtures were divided into two cultures with one of them being treated with 3 cycles of 5 Gy IR. Cell mixtures were then allowed to grow for 10 days and analyzed by flow cytometry to determine changes in abundance of each cell population. All quantification data represent mean ± SD from three independent experiments. *$p < 0.05$.